

## TRACER DIFFUSION IN SINTERED STAINLESS STEEL FILTERS: MEASUREMENT OF EFFECTIVE DIFFUSION COEFFICIENTS AND IMPLICATIONS FOR DIFFUSION STUDIES WITH COMPACTED CLAYS

MARTIN A. GLAUS<sup>1,\*</sup>, ROGER ROSSÉ<sup>1</sup>, LUC R. VAN LOON<sup>1</sup>, AND ANDRIY E. YAROSHCHUK<sup>2</sup>

<sup>1</sup> Laboratory for Waste Management, Paul Scherrer Institut, CH-5232 Villigen, Switzerland

<sup>2</sup> ICREA and Departament d'Enginyeria Química (EQ), Universitat Politècnica de Catalunya, 08028 Barcelona, Spain

**Abstract**—The use of porous filters is indispensable in laboratory- and field-scale diffusion studies, where sample confinement is needed for mechanical reasons. Examples are diffusion studies with compacted swelling clays or brittle clay stones. Knowledge of the diffusion properties of these filters is important in cases where they contribute significantly to the overall diffusive resistance in the experimental setup. In the present study, measurements of effective diffusion coefficients ( $D_b$ ) in porous, stainless steel filter discs are reported for tritiated H<sub>2</sub>O (HTO), <sup>22</sup>Na<sup>+</sup>, Cs<sup>+</sup>, and Sr<sup>2+</sup> before and after use of the filters in diffusion experiments with different clay minerals. The  $D_b$  values for used filters were found to be less than those of the as-received filters by ~30–50%. The  $D_b$  values measured for the diffusion of HTO, <sup>22</sup>Na<sup>+</sup>, Cs<sup>+</sup>, and Sr<sup>2+</sup> in unused and used stainless steel filter discs correlated fairly well with the respective molecular diffusion coefficients in bulk water. Although such correlations are inherently associated with some uncertainties, they allow reasonable estimates to be made for diffusants for which no  $D_b$  values are available. For the first time, a procedure is outlined that allows an integrative assessment to be made for the impact of the uncertainties in the filter diffusion properties on the combined standard uncertainties of the diffusion parameters obtained from through-diffusion experiments. This procedure can be used in the design and optimization of through-diffusion experiments in which the diffusive resistance of the porous filters must not be ignored. Shown here, as a general rule of thumb, is that, if the effective diffusion coefficient in the porous filter is at least three times larger than that in the clay, the choice of geometrical boundary conditions is rather uncritical, as long as the thickness of the clay sample is greater than that of the porous filters.

**Key Words**—Clay, Diffusion, Filter, Mass Transfer, Optimization, Porous Media.

### INTRODUCTION

Porous stainless steel filters are frequently used in diffusion studies in which the diffusant is supplied from a solution reservoir to a confined solid or crushed rock sample. They are indispensable for diffusion studies with strongly expanding clays, such as bentonite, or in cases where the rock sample disintegrates upon contact with the solution. Typical applications of porous filters range from laboratory through-diffusion studies (*e.g.* Oscarson, 1994; Molera and Eriksen, 2002; Shackelford, 1991), where the filters are typically used in a sandwich-type arrangement, *i.e.* filter–clay–filter, up to field-scale diffusion studies, where the tracer solution in a packed borehole is brought into contact with the surrounding rock by a porous steel filter lining (Wersin *et al.*, 2004). For a proper evaluation of the clay diffusion coefficients in such experiments, knowing the diffusive properties of the tracers in these filters is important. Owing to the geometric differences in the pore structure of the filters and the clays, the diffusive

resistance of the filters is negligible in many cases. However, no clear criteria have been formulated for deciding under which conditions filter effects can be ignored. Many authors do not state explicitly whether and how they included filter effects in the calculation of clay-diffusion coefficients. Filter effects can typically be ignored in experiments with clay stones where the effective diffusion coefficients are small because of the small porosities of these solids (*e.g.* Van Loon *et al.*, 2005). However, in cases where the diffusive resistances of clay and filter are similar (*e.g.* Glaus *et al.*, 2007), the diffusive flux through the clay may be strongly affected by the filters. The thicknesses of the clay sample and filters must be optimized according to their diffusivities so that experiments can be carried out on a reasonable time scale and with reasonable accuracy.

The need for diffusion data for fresh and used filters was recognized a long time ago (van Schaik *et al.*, 1966). However, literature data on effective diffusion coefficients for porous stainless steel filters are scarce (Bourke *et al.*, 1990; Molera and Eriksen, 2002) and were measured for unused filters only. Note that filters might be exposed to pressures of several tens of MPa in a diffusion experiment with highly compacted, strongly swelling clays such as bentonites (Madsen, 1998). The mechanical stress may change the pore geometry of the

\* E-mail address of corresponding author:

[martin.glaus@psi.ch](mailto:martin.glaus@psi.ch)

DOI: 10.1346/CCMN.2008.0560608

filters, or the filters may get clogged leading to a potential increase in their diffusive resistance. No data on diffusion in used porous stainless steel filters are available in the literature as yet. It has to be assumed that literature values obtained for diffusion in clays may be biased when simply correcting for the diffusive properties of unused filters.

The purpose of the present work is to measure the diffusive properties of porous stainless steel filters for a series of diffusants before and after use of the filters in diffusion experiments with various clay minerals. Na-conditioned montmorillonite (*Na-mom*), Volclay (*volc*, a Na-bentonite), Na-conditioned illite (*Na-ill*), and kaolinite (*kao*) were chosen as typical representatives of strongly swelling and non-swelling clays. Owing to the high concentration of fixed negative charges ( $\sim 0.8$  eq kg<sup>-1</sup>), *Na-mom* and *volc* produce the greatest swelling pressures, whereas for *kao* (cation exchange capacity, CEC = 0.03–0.04 eq kg<sup>-1</sup>) little or no swelling occurs. *Na-ill* is in between these two extremes (CEC  $\approx 0.1$  eq kg<sup>-1</sup>). The results will be discussed with a view to the optimization of the experimental setup and to the impact of the uncertainties in the filter properties on the combined standard uncertainties involved in the calculation of the diffusion parameters for the clays.

## METHODS

### *Reagents, samples, and analytical procedures*

The materials and procedures used were described by Glaus *et al.* (2007). The illite originated from le Puy (France) and was adjusted to the Na form (see Glaus *et al.*, 2007). Volclay was purchased from Südchemie (Germany) and used as received. Porous, stainless steel filters (stainless steel: 316 L, pore diameter: 10  $\mu$ m, disc diameter: 25.4 mm, thickness 0.16 $\pm$ 0.01 mm) were purchased from MOTT industrial division (Farmington, Connecticut, USA). The Darcy hydraulic conductivity for water of these filters was determined to be  $\sim 2 \times 10^{-5}$  m s<sup>-1</sup> at 295 K. In view of the colloidal character of many clays, the intrusion of filter pores by clay particles cannot be avoided, even if using filters with smaller pore sizes. However, for clays >5 mm thick, the loss of clay and the associated possible changes in the degree of compaction can be tolerated with the porous filters used.

Concentrations of Cs<sup>+</sup> and Sr<sup>2+</sup> were measured by high-performance cation exchange chromatography (HPCEC) using a Dionex DX-600 system (Dionex, Switzerland) consisting of a metal-free GP50-2 quaternary gradient pump, a CD25 conductivity detector, and an AS50 autosampler, equipped with a 9750 motor-driven Rheodyne injection valve and a 50  $\mu$ L PEEK injection loop. A 4 mm  $\times$  250 mm Ionpac CS12 separation column together with a 4 mm  $\times$  50 mm Ionpac CG12 guard column (Dionex, Switzerland) was used for separation. 50  $\mu$ L samples were injected in the full loop mode. The

eluent was 18 mM methanesulfonic acid operated at a flow rate of 1 cm<sup>3</sup> min<sup>-1</sup>. Standard solutions of Cs<sup>+</sup> and Sr<sup>2+</sup> containing the same concentrations of Na<sup>+</sup> as in the samples were used for calibration.

The activities of HTO and <sup>22</sup>Na were measured simultaneously by liquid scintillation on a Tri-carb 2250 CA counter (Cammerra-Packard) in homogenized mixtures containing 10 cm<sup>3</sup> each of sample and scintillation cocktail (Ultima Gold XR, Cammerra-Packard). For the activity measurement of mixtures containing the two isotopes, the scintillation measurements were carried out in two energy windows (window A: 0–9 keV, window B: 9–160 keV). The activities of HTO ( $a_{\text{HTO}}$ ) and <sup>22</sup>Na ( $a_{\text{Na}}$ ) were calculated from:

$$a_{\text{HTO}} = \frac{N^{\text{A}} - Q_{\text{Na}} \cdot N^{\text{B}}}{60 \cdot (f_{\text{HTO}}^{\text{A}} - Q_{\text{Na}} \cdot f_{\text{HTO}}^{\text{B}})} \quad (1)$$

$$a_{\text{Na}} = \left( N^{\text{B}} - \frac{N^{\text{A}} - Q_{\text{Na}} \cdot N^{\text{B}}}{Q_{\text{HTO}} - Q_{\text{Na}}} \right) \cdot \frac{1}{60 \cdot f_{\text{Na}}^{\text{B}}} \quad (2)$$

where:  $N^{\text{A}}$  and  $N^{\text{B}}$  are counting rates (cpm) in windows A and B;  $f_{\text{HTO}}^{\text{A}}$  and  $f_{\text{HTO}}^{\text{B}}$  are counting efficiencies (cpm Bq<sup>-1</sup>) of HTO in windows A and B determined independently using standards with known activities; and  $f_{\text{Na}}^{\text{A}}$  and  $f_{\text{Na}}^{\text{B}}$  are counting efficiencies (cpm Bq<sup>-1</sup>) of <sup>22</sup>Na in windows A and B determined independently using standards with known activities.

$$\begin{aligned} Q_{\text{H}_2\text{O}} &= f_{\text{HTO}}^{\text{A}}/f_{\text{HTO}}^{\text{B}} \\ Q_{\text{Na}} &= f_{\text{Na}}^{\text{A}}/f_{\text{Na}}^{\text{B}} \end{aligned}$$

In practice, because the counting efficiency for HTO in window B is virtually zero, equations 1 and 2 reduce to:

$$a_{\text{HTO}} = \frac{N^{\text{A}} - Q_{\text{Na}} \cdot N^{\text{B}}}{60 \cdot f_{\text{HTO}}^{\text{A}}} \quad (3)$$

$$a_{\text{Na}} = \frac{N^{\text{B}}}{60 \cdot f_{\text{Na}}^{\text{B}}} \quad (4)$$

Uncertainties for  $a_{\text{HTO}}$  and  $a_{\text{Na}}$  were calculated by error propagation of the uncertainties involved in the counting statistics ( $N^{\text{A}}$  and  $N^{\text{B}}$ ) and the observed variances of the counting efficiencies.

### *Diffusion measurements*

Through-diffusion measurements were carried out using 'in-house' manufactured acrylic glass diffusion cells consisting of two chambers, each of 115 cm<sup>3</sup>, separated by the filter disc. The filters were supported laterally with FKM-elastomer (Angst + Pfister, Switzerland) flat seals in order to prevent advective transport around the filters or liquid loss from the diffusion cells. The solutions were stirred magnetically to maintain homogeneity in the solutions. Owing to the relatively large hydraulic conductivity of the filters, great care was taken to avoid any differences in

hydraulic head between the two chambers when adding or withdrawing samples.

Filters were used either 'as received' from the manufacturer (unused filters) or taken from diffusion experiments with the various clays as described by Glaus *et al.* (2007) after contact times from 30 days up to 400 days (used filters). Any clay sticking to the filter surface was removed mechanically before use. Filter-diffusion measurements were carried out in NaClO<sub>4</sub> solutions at various concentrations. The mechanical deformation of the filters in experiments with strongly expanding clays, *viz.* *Na-mom* and *volc*, was visible as a tiny imprint in the filter of the contours of the channel in the steel-retaining end-plate of the diffusion cells (*cf.* Figure 1). Before use, the filter discs were saturated with the same medium as used in the filter diffusion experiments. After filling the chambers with NaClO<sub>4</sub> solution, the diffusion cells were evacuated in a desiccator for ~15 min in order to remove any air trapped in the pore space of the filter discs or the apparatus. Diffusion was started by adding ~500 µL of a concentrated solution of the diffusant to one of the chambers. HTO and <sup>22</sup>Na were used as radioactive tracers, whereas concentrations of the stable isotopes of Cs and Sr were analyzed by ion chromatography.

Effective diffusion coefficients of the filter discs ( $D_b$ ) were calculated from the total amount of diffused tracer,  $n_t$  (mol), accumulated as a function of time on the 'low-concentration' side of the diffusion cell according to:

$$D_b = \frac{a \cdot L_b}{S \cdot C_0} \quad (5)$$

where  $a$  is the slope of the linear part (constant flux) of the plot of  $n_t$  as a function of time (s),  $L_b$  the thickness of the filter disc (m),  $S$  the cross-sectional area of the filter

disc (m<sup>2</sup>), and  $C_0$  is the initial concentration (mol m<sup>-3</sup>) in the 'high-concentration' reservoir. Linear-weighted regression was used to calculate  $a$ . Data in the transition diffusion region of the experiments, usually between 0 and 1 h, were omitted from regression. The change in concentration in the 'high concentration' reservoir due to diffusive loss of the tracer under study was verified to be not larger than 3%, and the maximum concentration in the 'low-concentration' reservoir did not exceed 3% of the initial concentration in the 'high-concentration' reservoir, thus justifying the assumption of constant boundary conditions in the data evaluation. Note that in most cases calculation of reliable values for the filter porosity from the diffusion data was impossible due to the rapid breakthrough of the tracer.

#### *Standard uncertainties of individual data points and mean values*

Combined standard uncertainties for a single data point were calculated based on known statistical and non-statistical uncertainties according to the recommendations given by the EURACHEM Working Group (Williams *et al.*, 1995). In some cases discrepancies between these combined standard uncertainties and the scatter of repeat measurements were observed. The standard uncertainty of the individual measurements and the pooled standard uncertainty (Gold, 1997) based on the combined standard uncertainties of the individual measurements were compared. The larger value of the latter two quantities was used as the combined standard uncertainty of the mean of repeat measurements.

## RESULTS AND DISCUSSION

### *Effective diffusion coefficients of porous filters*

Breakthrough curves for the through-diffusion of Sr for an unused filter and one which had previously been used in a diffusion experiment with various clays compacted to a dry density of ~1950 kg m<sup>-3</sup> were compared (Figure 2). For the unused filter, a  $D_b$  value of  $(1.1 \pm 0.1) \times 10^{-10}$  m<sup>2</sup> s<sup>-1</sup> was calculated. This value was reduced to  $(0.61 \pm 0.02) \times 10^{-10}$  m<sup>2</sup> s<sup>-1</sup> for filters used previously in experiments with *Na-mom*, to  $(0.50 \pm 0.04) \times 10^{-10}$  m<sup>2</sup> s<sup>-1</sup> for filters used with *Na-ill*, and  $(0.79 \pm 0.02) \times 10^{-10}$  m<sup>2</sup> s<sup>-1</sup> for those used in experiments with *kao*. The increased diffusive resistance of used filter discs may be explained by: (1) the mechanical stress induced by the expanding clay leads to distortions in the original pore geometry, or (2) small clay particles infiltrate the pores in the filters also, leading to changes in the geometry of diffusion paths (*viz.* changed constrictivity or tortuosity). The second interpretation is favored by the experimental findings because *Na-mom* and *kao* differ considerably in their swelling behavior. The increase in diffusive resistance of the filters was further observed to be largely independent of the clay thickness used in the preceding diffusion experiment

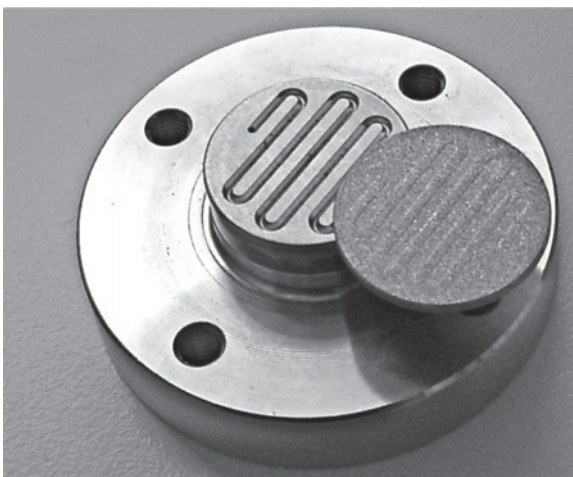


Figure 1. End plate of a diffusion cell and porous steel filter after an experiment with a 10 mm thick sample of *Na-mom*. The filter was pushed against the end plate by the pressure of the expanding clay leaving a tiny imprinted structure (height ~0.03 mm) from the channel system for the circulating fluid.

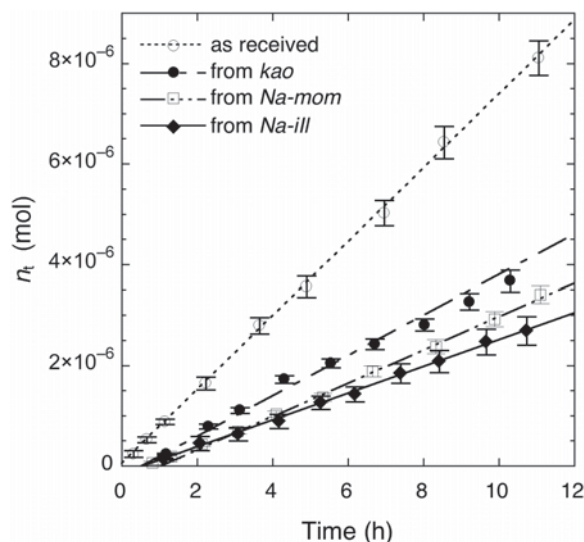


Figure 2. Comparison of breakthrough curves for  $\text{Sr}^{2+}$  through filters used as received or after previously being in contact with the clays.

with clay (data not shown), while the mechanical deformation of the filters (*cf.* Figure 1) was clearly less for thin clay samples. Based on the height of the imprint, a 1.6 mm thick filter was compressed by  $\sim 0.03$  mm after use with a 10 mm thick sample of *Na-mom*. This corresponds to a relative decrease in the porosity of  $\sim 2\%$ . An empirical relationship for diffusion in porous media (Boving and Grathwohl, 2001) relates  $D_b$  to the molecular diffusion coefficient in bulk water ( $D_w$ ) by:

$$D_b = D_w \varepsilon^m \quad (6)$$

where  $m$  is an empirical parameter and  $\varepsilon$  is the porosity. Using  $D_w = 7.9 \times 10^{-10}$  (Li and Gregory, 1974) for Sr and a porosity of 0.285 for unused porous steel filters,  $m$  was estimated to be 1.6 for the diffusion of Sr through such filters. According to equation 6,  $D_b$  would decrease by  $\sim 3\text{--}4\%$  for a decrease in porosity of 2%. The observed decrease in  $D_b$  was, however,  $\sim 45\%$  after using the filters with *Na-mom*. This again tends to support the second proposed explanation above. Gravimetric measurements further demonstrated that only small parts of the filter porosity were filled with clay. The loss of clay to the filters is, therefore, so low that the diffusion results for the compacted clay are only marginally influenced by the decrease in the degree of compaction, even when using clay samples with thicknesses in the millimeter range.

With respect to using filter diffusion data in the evaluation of clay diffusion data, verifying that the diffusive properties of the filters remain constant during diffusion experiments with the clays is important. When setting up such experiments, the clays are usually equilibrated with the contacting fluid for typically 1 month before the tracer is added. To investigate

whether or not any time-dependent effects occur,  $D_b$  values obtained after a contact time of  $\sim 30$  days were compared to  $D_b$  values measured after much longer contact times. An overview of such data with the corresponding initial values of fresh filters is given in Table 1 for HTO,  $^{22}\text{Na}^+$ ,  $\text{Cs}^+$ , and  $\text{Sr}^{2+}$ . No values for the rock capacity factors (denoted in the following as  $\alpha$ :  $\alpha = \varepsilon + \rho R_d$ , where  $\rho$  is the dry bulk density of the solid and  $R_d$  the sorption distribution ratio of the tracer between the solid and the liquid phase) are reported (Table 1) because these could not be determined with sufficient accuracy with the experimental setup used. The combined standard uncertainties specified in Table 1 include uncertainties due to the experimental and analytical procedures as well as the variability found for a series of nominally 'identical' filter discs from a single production lot. Even larger variations (up to 20–30%) were measured between filter discs from different production lots. The data reported here (Table 1) lead to the conclusion that the increase in diffusive resistance of the filter discs occurred within the first 30 days of contact time between the compacted clay and the circulating fluid. No measurable dependence of  $D_b$  values on the salt concentration in the range 0.1 and 1.0 M  $\text{NaClO}_4$  could be observed for filters in the unused state. For used filters the values specified in Table 1 hold for salt concentrations between 0.5 and 1.0 M  $\text{NaClO}_4$ . For 0.1 M  $\text{NaClO}_4$ , slightly increased  $D_b$  values ( $\sim 20\%$ ) were measured for  $\text{Na}^+$  and  $\text{Sr}^{2+}$ .

The effective diffusion coefficients for tracers through filter discs correlate fairly well with their respective  $D_w$  values (Figure 3a,b). Such values and their dependence on temperature were given by Li and Gregory (1974). The correlations established in Figure 3a,b may be useful for estimating the diffusive resistance of porous steel filter discs toward diffusants for which no experimental data are available. Note that the diffusion of HTO decreased more pronouncedly in used filters than the diffusion of cations. This may be caused by the fast diffusion of cations in compacted swelling clays owing to increased tracer gradients across the interlayer space, as demonstrated for the diffusion of  $\text{Na}^+$  and  $\text{Sr}^{2+}$  in compacted *Na-mom* (Glaus *et al.*, 2007). Interestingly,  $\text{Cs}^+$  shows a delayed breakthrough in filter discs that had previously been in contact with compacted *Na-mom* as compared to unused ones (*cf.* Figure 4). An  $\alpha$  value of 1.8 was calculated in this experiment with an unusually small relative uncertainty of  $\sim 10\%$ , whereas  $\alpha$  values for  $\text{Na}^+$  and  $\text{Sr}^{2+}$  were distinctly  $< 1$ . All these observations again corroborate the hypothesis that the change in diffusion properties of filter discs used in diffusion experiments with compacted clays are mainly due to infiltration of clay particles into the filter pores. The comparably faster diffusion of cations as compared to neutral species and the delayed breakthrough of  $\text{Cs}^+$ , the most strongly sorbing cation among the diffusants tested here, are characteristic for diffusion in clay.

Table 1. Overview of best-fit parameter values for effective diffusion coefficients in porous stainless steel filter discs ( $D_b$ ) at  $20 \pm 2^\circ\text{C}$ .

Diffusant	Fresh filter discs		Used filter discs <sup>a</sup> after 30 days' contact with clay		Used filter discs <sup>a</sup> after contact time with clay as indicated		$t_c$ (days) <sup>d</sup>
	$D_b$ ( $\text{m}^2 \text{s}^{-1}$ ) <sup>b</sup>	$n^c$	$D_b$ ( $\text{m}^2 \text{s}^{-1}$ ) <sup>b</sup>	$n^c$	$D_b$ ( $\text{m}^2 \text{s}^{-1}$ ) <sup>b</sup>	$n^c$	
HTO	$(23 \pm 2.5) \times 10^{-11}$	18	$(10.9 \pm 2.2) \times 10^{-11}$ (Na-mom)	6	$(12.0 \pm 1.0) \times 10^{-11}$ (Na-mom)	2	40
<sup>22</sup> Na <sup>+</sup>	$(16 \pm 1.6) \times 10^{-11}$	18	$(9.1 \pm 1.8) \times 10^{-11}$ (Na-mom)	6	$(8.8 \pm 1.1) \times 10^{-11}$ (Na-mom)	8	140–200
<sup>134</sup> Cs <sup>+</sup>	$(20 \pm 2.5) \times 10^{-11}$	4	$(14.0 \pm 2.7) \times 10^{-11}$ (Na-mom)	6	$(8.2 \pm 1.4) \times 10^{-11}$ (volc <sup>e</sup> )	6	120
<sup>85</sup> Sr <sup>2+</sup>	$(10 \pm 1.1) \times 10^{-11}$	21	$(6.5 \pm 1.3) \times 10^{-11}$ (Na-mom)	6	not determined	18	~400
<sup>85</sup> Sr <sup>2+</sup>					$(5.2 \pm 0.5) \times 10^{-11}$ (Na-ill)	3	~250
<sup>85</sup> Sr <sup>2+</sup>					$(5.7 \pm 0.4) \times 10^{-11}$ (volc <sup>e</sup> )	6	~180
<sup>85</sup> Sr <sup>2+</sup>					$(7.7 \pm 0.2) \times 10^{-11}$ (kaol)	2	~100

<sup>a</sup> Used filter discs were taken after being contacted with clays compacted to a dry bulk density of  $1950 \pm 50 \text{ kg m}^{-3}$ . The type of clay is indicated in parentheses.

<sup>b</sup> Fresh filters: values for 0.1–1.0 M NaClO<sub>4</sub>; used filters: values for 0.5–1.0 M NaClO<sub>4</sub>. Slightly increased values were observed for used filters at lower salt concentrations (cf. the text).

<sup>c</sup> Number of replicates.

<sup>d</sup> Contact time with clay.

<sup>e</sup> Volclay is a bentonite.

Combined standard uncertainties for effective clay diffusion coefficients

For the estimation of the combined standard uncertainties of the diffusion parameters in clay, the effective diffusion coefficient ( $D_e$ ), and the rock capacity factor ( $\alpha$ ), the uncertainties in the diffusive properties of the filter discs must be taken into account. Because an analytical solution is available for the diffusion through a sandwich-type filter–clay–filter arrangement

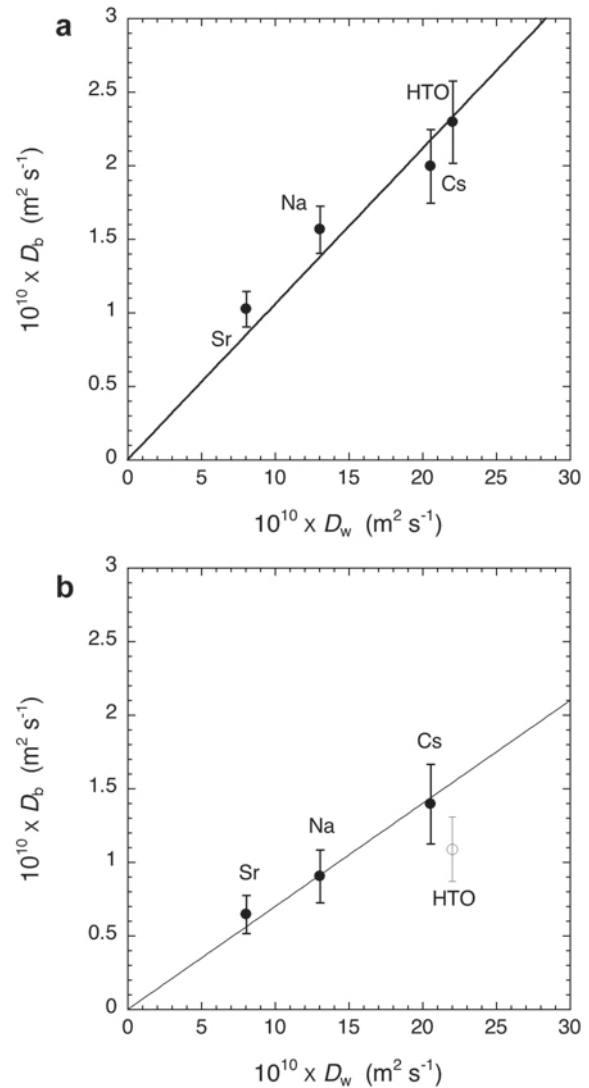


Figure 3. (a) Relationship between effective diffusion coefficients measured for fresh filters ( $D_b$ ) with their corresponding molecular diffusion coefficients in bulk water ( $D_w$ ). The regression line was forced through the origin. (b) Relationship between  $D_b$  values used in diffusion experiments with compacted Na-mom, with their corresponding molecular diffusion coefficients in bulk water  $D_w$  values. The measurement for HTO (open circle) was not included in the regression. The regression line was forced through the origin.

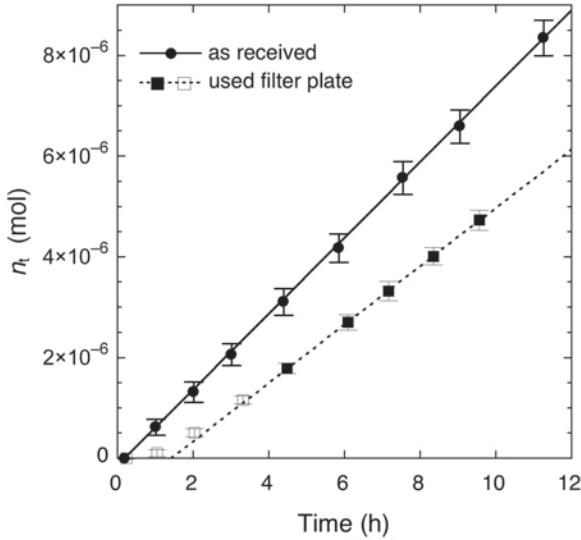


Figure 4. Comparison of breakthrough curves for  $\text{Cs}^+$  through fresh and used filters (*Na-mom*). Mass data for the used filters were normalized in order to simulate identical concentration gradients for the two experiments (initial concentrations of 3.3 mM). Filled symbols denote the data used for regression, open symbols, those not used for regression.

(Yaroshchuk *et al.*, 2008), these uncertainties are estimated here using error propagation. For a steady-state flux and constant concentration boundary conditions, the concentration-normalized flux ( $F$ ,  $\text{m s}^{-1}$ ) at the low-concentration boundary becomes (*cf.* equation 33 in Yaroshchuk *et al.*, 2008):

$$F \equiv \frac{j_s}{C_0} = \frac{D_b}{(2+h)L_b} \quad (7)$$

where  $j_s$  is a steady-state flux ( $\text{mol m}^{-2} \text{s}^{-1}$ ); and  $D_b$  is the effective diffusion coefficient of the porous filters. In Yaroshchuk *et al.* (2008), the permeability coefficient,  $P_b = D_b/L_b$  (with  $L_b$  being the thickness of the filter disc) is generally used instead of  $D_b$ .  $C_0$  is the tracer concentration in the source reservoir ( $\text{mol m}^{-3}$ );  $h$  is a parameter defined by the thickness ( $L_c$ ) of the clay sample (m), the effective diffusion coefficients in the clay sample, and the boundary layers, according to:

$$h \equiv \frac{L_c D_b}{L_b D_e} \quad (8)$$

For the case of identical thicknesses of the two confining filters, substitution of equation 8 into equation 7 yields:

$$D_e = \frac{j_s L_c D_b}{C_0 D_b - 2j_s L_b} \quad (9)$$

According to error propagation, the combined standard uncertainty of  $D_e$  ( $u_c(D_e)$ ) can be calculated from:

$$u_c(D_e) = \sqrt{\sum_{i=1}^n \left( \frac{\partial D_e}{\partial x_i} \right)^2 (\Delta x_i)^2} \quad (10)$$

where  $x_i$  are the (uncorrelated) variables in equation 9 and  $\Delta x_i$  their relative standard uncertainties.

Similarly, the combined standard uncertainty of  $\alpha$  ( $u_c(\alpha)$ ) is obtained from the Fourier-transform solution (Yaroshchuk *et al.*, 2008) by using the expression for the dimensional breakthrough time,  $t_{bt}$  (*cf.* equation 38 in Yaroshchuk *et al.*, 2008), defined as the intercept of abscissa by the extension of the linear part of the data in a plot of accumulated amount in the ‘low-concentration reservoir’ vs. elapsed time:

$$t_{bt} = \frac{\alpha}{6D_e} L_c^2 \frac{1 + 3r + \frac{3}{2}r^2}{1+r} \quad (11)$$

where

$$R \equiv \frac{2}{h} \quad (12)$$

Combining equations 8, 9, 11, and 12 leads to:

$$\alpha = \frac{6j_s t_{bt} C_0 D_b^2}{L_c C_0^2 D_b^2 + 2L_b L_c C_0 D_b j_s - 2L_c L_b^2 j_s^2} \quad (13)$$

Expressions for the partial derivatives in equation 10 used for the calculation of  $u_c(D_e)$  and  $u_c(\alpha)$  are given in the Appendix. From the definition of equations 9 and 13, these equations hold strictly for constant-concentration boundary conditions only. However, the error propagation proposed here can also be applied for non-stationary boundary conditions under the condition that the concentration changes at the high-concentration boundary proportionally affect the quasi-steady-state flux observed at the low-concentration boundary. In such cases the flux data may be renormalized according to the changes in the high-concentration reservoir, leading to a linear relationship between accumulated mass vs. elapsed time. Quantitative criteria for this condition to be fulfilled were obtained by Yaroshchuk *et al.* (2008). In such cases  $C_0$  may simply be replaced in the equations by a time-dependent value for the concentration at the high-concentration boundary,  $C_t$ . The uncertainties involved in the ‘renormalization’ of the  $C_t$  data (for guidance on how to estimate these, the reader is referred to Yaroshchuk *et al.*, 2008) need to be considered adequately in the error propagation.

#### Optimization of the experimental setup

In view of the preceding section, the ratio of effective diffusion coefficients in filter and clay ( $D_b/D_e$ ) and the ratio of the respective thicknesses ( $L_b/L_c$ ) are useful quantities for the discussion of  $u_c(D_e)$  and  $u_c(\alpha)$ . It is interesting to examine how these combined standard

uncertainties develop for fixed values of  $D_b/D_e$  and variations in  $L_b/L_c$ , as the experimenter is free to choose the thickness of the clay sample – and to some degree the thickness of the porous filters.

In a first step, the result of ignoring the impact of confining filters is demonstrated using published data (Glaus *et al.*, 2007) for the diffusion of  $\text{Na}^+$  in *Na-mom* at a dry bulk density of  $1900 \text{ kg m}^{-3}$  as a case example. These data were measured as a function of varying salt concentration in the liquid phase being in contact with the clay (denoted in the following as the ‘external salt concentration’). The tracer concentration gradient in the pore space of the clay, the driving force for diffusion, depends on the external salt concentration (Glaus *et al.*, 2007). Increasing the external salt concentrations led to weaker sorption of the trace cations and to smaller tracer concentration gradients in the pore space of the clay. As a consequence, the effective diffusion coefficients in the clay became dependent on the external salt concentration, while  $D_b$  values for porous filters exhibited no such dependence (*cf.* Table 1). Table 2 shows a comparison of the  $D_e$  values calculated by taking into account the diffusive resistance of the filters with those calculated by ignoring the effect of the filters. The conditions relevant for the measurement of  $D_e$  values for  $^{22}\text{Na}^+$  diffusion in *Na-mom* (Glaus *et al.*, 2007) are also shown in Table 2. The values of  $D_e$  (Table 2) are systematically underestimated when ignoring the diffusive resistance of the filters and the deviation from the correct value increased in those cases, in which the effective diffusion coefficients for filters and clay were similar. However, when the  $L_b/L_c$  ratios were sufficiently small and the  $D_b/D_e$  ratios sufficiently large, the error of ignoring the diffusive resistance became tolerable in view of other error sources, such as the analytical errors.

For this reason it is important to integrate a second step into the discussion of uncertainties due to the use of confining filters into the overall discussion of  $u_c(D_e)$  and  $u_c(\alpha)$  (*cf.* equation 10 and the respective expression for

$u_c(\alpha)$ ). A simulation of the relative combined standard uncertainty of calculated  $D_e$  values,  $u_c(D_e)/D_e$ , as a function of  $D_b/D_e$  for three different ratios of  $L_b/L_c$  and the data shown in Table 2 is given in Figure 5a. For simplicity the simulation assumed that  $\Delta x_i$  values are independent of the absolute values of  $x_i$ , *i.e.* the same relative uncertainty was applied for a single variable throughout. Hence the values of the series in equation 10 are, for a given ratio  $L_b/L_c$ , independent of the absolute values of  $L_b$  and  $L_c$ , and the calculated  $u_c(D_e)$  values are

Table 2. Impact of ignoring the diffusive resistance of confining filters on the resulting values for diffusion in the clay sample ( $D_e$ ) using measurements of  $^{22}\text{Na}^+$  diffusion in compacted *Na-mom* (Glaus *et al.*, 2007).

[NaClO <sub>4</sub> ] (M) <sup>a</sup>	$L_b/L_c$	$D_e$ (m <sup>2</sup> s <sup>-1</sup> ) Filters ignored <sup>b</sup>	$D_e$ (m <sup>2</sup> s <sup>-1</sup> ) Filters taken into account <sup>c</sup>
0.1	0.29	$1.2 \times 10^{-10}$	$3.7 \times 10^{-10}$
0.5	0.29	$5.9 \times 10^{-11}$	$8.6 \times 10^{-11}$
0.7	0.29	$3.9 \times 10^{-11}$	$5.3 \times 10^{-11}$
1.0	0.29	$3.0 \times 10^{-11}$	$3.8 \times 10^{-11}$
1.0	0.16	$3.1 \times 10^{-11}$	$3.4 \times 10^{-11}$

<sup>a</sup> External salt concentration.

<sup>b</sup> Assumption:  $D_b \gg 8.6 \times 10^{-11} \text{ m}^2 \text{ s}^{-1}$ .

<sup>c</sup>  $D_b = 8.6 \times 10^{-11} \text{ m}^2 \text{ s}^{-1}$  (*cf.* Table 1).

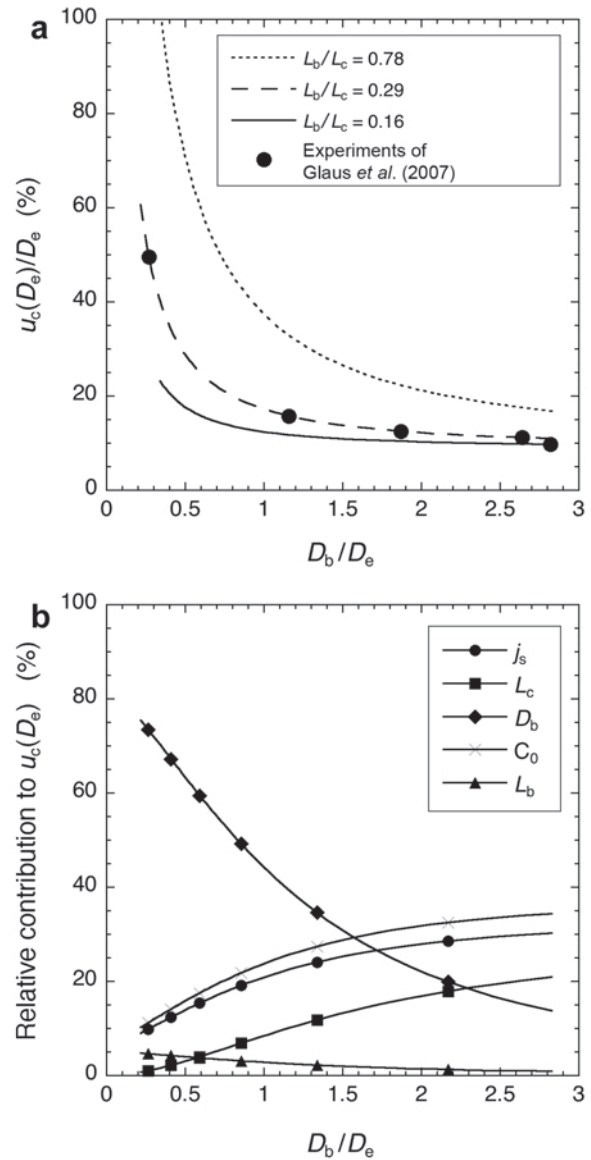


Figure 5. (a) Simulation of the relative combined standard uncertainty in the calculation of  $D_e$  as a function of the ratio of effective diffusion coefficients for filter and clay ( $D_b/D_e$ ) and the ratio of diffusion length in filter and clay ( $L_b/L_c$ ). (b) Relative contribution of the individual uncertainties of  $j_s$ ,  $L_b$ ,  $L_c$ ,  $D_b$ , and  $C_0$  to  $u_c(D_e)$  for the simulation in Figure 5a with  $L_b/L_c = 0.29$ .

universally valid for the assumed  $\Delta x_i$  values. The values used for the simulation were 5% for  $\Delta j_s$  and  $C_0$  and 25% for  $\Delta D_b$ . As shown in Tables 1 and 2, systematic errors >35% may be introduced if  $D_b$  values for unused instead of used filters are applied. Ignoring the impact of the swelling of clays on the diffusion properties of the porous filters may therefore lead to even greater  $u_c(D_e)/D_e$  values than those shown in Figure 5a (*cf.* Table 2). Results presented in Figure 5a lead to the conclusion that, for a given ratio of  $D_b/D_e$ ,  $u_c(D_e)/D_e$  becomes optimal for small ratios of  $L_b/L_c$ . However, parameter ranges exist in which the choice of  $L_b/L_c$  is not critical. This is the case for  $L_b/L_c < 0.3$  provided that  $D_b/D_e > 1.5$ . In these ranges the contribution of  $\Delta D_b$  does not contribute significantly to the value of  $u_c(D_e)$ . This is illustrated for the case of  $L_b/L_c = 0.29$  in Figure 5b, which shows the contribution of the individual sources of uncertainty, *i.e.*  $j_s$ ,  $L_b$ ,  $L_c$ ,  $D_b$ , and  $C_0$  (*cf.* equations A3–A7 in the appendix), as a function of the ratio  $D_b/D_e$ . Only for  $D_b/D_e < \sim 1.5$  does  $\Delta D_b$  become the dominant source of uncertainty. Such ratios are typically encountered when dealing with cation diffusion in highly compacted, swelling clays (*cf. e.g.* Glaus *et al.*, 2007), or with the diffusion of uncharged (*e.g.* HTO) or positively charged species in clays with low tortuosities and high constrictivities. For such cases, a suitable choice of  $L_b/L_c$  is critical. According to Figure 5a, a maximum value of  $L_b/L_c \approx 0.3$  should not be exceeded, otherwise  $u_c(D_e)/D_e$  values >20% have to be accepted. Further, for  $D_b/D_e > \sim 3$  the choice of  $L_b/L_c$  is rather uncritical, as long as the clay sample is thicker than the porous filters. Note that, in general, the best choice of  $L_b/L_c$  does not only depend on the expected value for  $u_c(D_e)$ . The duration of through-diffusion experiments is also a crucial issue, particularly when dealing with strongly sorbing tracers. The time needed to reach steady-state conditions increases with the square of the diffusion length. Time may be restricted in the sense of project duration, but also with the sensitivity of measurement, because the decay of radioactive isotopes may set limits to the maximum duration of a through-diffusion experiment. Because of this, conflicting interests may arise. In view of small  $u_c(D_e)$  values, thick clay samples are preferable. However, thin samples are desirable in view of the restrictions with the duration of the experiments. If the expected clay diffusion coefficients are known to a rough order of magnitude in the planning phase of an experiment, a careful optimization of the geometry with the help of equation 10 may avoid time-consuming evaluations of the optimum conditions for the measurement.

Similarly the influence of the geometry of diffusion equipment on  $u_c(\alpha)$  needs to be discussed. The situation is much simpler in that  $D_e$  does not appear in the partial derivatives of  $\alpha$  (*cf.* equations A10–A15 in the appendix). Calculated  $u_c(\alpha)$  values are therefore constant for any chosen ratio of  $D_b/D_e$ . Furthermore, for the ratios of

$L_b/L_c$  used for the simulation in Figure 5a,  $u_c(\alpha)$  is almost invariant. Consequently, the choice of the experimental setup is almost uncritical with respect to the determination of  $\alpha$ .

## CONCLUSIONS

The present work gives quantitative guidelines for taking into account the diffusive resistances of porous filter discs when performing diffusion experiments with compacted clay materials. Results and analysis revealed that effective filter diffusion coefficients need to be measured for an *in situ* state of the filters, because diffusion in such filters is decelerated as compared to fresh filters, probably because of clogging of the filter pores by the clays. Whether or not the filter discs play an important role in a diffusion experiment with compacted clays depends not only on the effective diffusive coefficients of filters and clay, but also on the geometry of the experimental setup. Equations 9 and 13 provide a simple method that may be implemented in a spreadsheet table to design the experimental setup appropriately. In cases where no experimental values for the effective diffusion coefficients for the filter discs are available, such data may be estimated from linear correlations with their molecular diffusion coefficients in bulk water. However, the relative standard uncertainties for diffusion in the filter discs may then be in the range 30–50%. The proposed procedure for taking into account these uncertainties into the combined standard uncertainties in the clay diffusion coefficients will help in deciding on whether or not such values may be acceptable for the precision required for the measurement of the diffusive properties of the clay.

## ACKNOWLEDGMENTS

The authors thank the Swiss National Cooperative for the Disposal of Radioactive Waste (NAGRA) for partially financing this work. Special thanks to F. Berger and M. Blumer (PSI) for their contribution to the design and construction of the diffusion cells.

## REFERENCES

- Bourke, P.J., Gilling, D., Jefferies, N.L., Lever, D.A., and Lineham, T.R. (1990) *Mass transfer through clay by diffusion and advection: description of intraval test case 1a. Safety studies*. Nirex Radioactive Waste Disposal NSS/R159.
- Boving, T.B. and Grathwohl, P. (2001) Tracer diffusion coefficients in sedimentary rocks: Correlation to porosity and hydraulic conductivity. *Journal of Contaminant Hydrology*, **53**, 85–100.
- Glaus, M.A., Baeyens, B., Bradbury, M.H., Jakob, A., Van Loon, L.R., and Yaroshchuk, A. (2007) Diffusion of  $^{22}\text{Na}$  and  $^{85}\text{Sr}$  in montmorillonite: Evidence of interlayer diffusion being the dominant pathway at high compaction. *Environmental Science and Technology*, **41**, 478–485.
- Gold, V. (1997) *Compendium of Chemical Terminology: IUPAC recommendations*. 2<sup>nd</sup> edition, Blackwell Scientific Publications, Oxford, UK.
- Li, Y.H. and Gregory, S. (1974) Diffusion of ions in sea water

- and in deep-sea sediments. *Geochimica et Cosmochimica Acta*, **38**, 703–714.
- Madsen, F.T. (1998) Clay mineralogical investigations related to nuclear waste disposal. *Clay Minerals*, **33**, 109–129.
- Molera, M. and Eriksen, T. (2002) Diffusion of  $^{22}\text{Na}^+$ ,  $^{85}\text{Sr}^{2+}$ ,  $^{134}\text{Cs}^+$  and  $^{57}\text{Co}^{2+}$  in bentonite clay compacted to different densities: experiments and modeling. *Radiochimica Acta*, **90**, 753–760.
- Oscarson, D. (1994) Surface diffusion: Is it an important transport mechanism in compacted clays? *Clays and Clay Minerals*, **42**, 534–543.
- Shackelford, C.D. (1991) Laboratory diffusion testing for waste disposal – a review. *Journal of Contaminant Hydrology*, **7**, 177–217.
- Van Loon, L.R., Baeyens, B., and Bradbury, M.H. (2005) Diffusion and retention of sodium and strontium in Opalinus clay: Comparison of sorption data from diffusion and batch sorption measurements, and geochemical calculations. *Applied Geochemistry*, **20**, 2351–2363.
- van Schaik, J.C., Kemper, W.D., and Olsen, S.R. (1966) Contribution of adsorbed cations to diffusion in clay-water systems. *Soil Science Society of America Proceedings*, **30**, 17–22.
- Wersin, P., Van Loon, L.R., Soler, J.M., Yllera, A., Eikenberg, J., Gimmi, T., Hernán, P., and Boisson, J.-Y. (2004) Long-term diffusion experiment at Mont Terri: first results from field and laboratory data. *Applied Clay Science*, **26**, 123–135.
- Williams, A., De Halleux, B., Diamondstone, B., Ellison, S., Haesselbarth, W., Kaarls, R., Mansson, M., Möller, H., Taylor, P., Thomas, B., Wegscheider, W., and Wood, R. (1995) *Quantifying Uncertainty in Analytical Measurement, first edition*. EURACHEM Working Group on Uncertainty in Chemical Measurement, Crown Copyright, London, UK.
- Yaroshchuk, A., Glaus, M.A., and Van Loon, L.R. (2008) Diffusion through confined media at variable concentrations in reservoirs: theory and experiment. *Journal of Membrane Science*, **319**, 133–140.
- (Received 22 May 2008; revised 2 September 2008; Ms. 0162; A.E. R. Dohrmann)

#### APPENDIX: PARTIAL DERIVATIVES

For the formation of the partial derivatives of equation 9, the following definitions are useful:

$$u = j_s L_c D_b \quad (\text{A1})$$

and

$$v = C_0 D_b - 2j_s L_b \quad (\text{A2})$$

The partial derivatives of  $D_e$  are then given as follows:

$$\frac{\partial D_e}{\partial j_s} = \frac{D_e}{j_s} + 2L_b \frac{u}{v^2} \quad (\text{A3})$$

$$\frac{\partial D_e}{\partial L_c} = \frac{D_e}{L_c} \quad (\text{A4})$$

$$\frac{\partial D_e}{\partial D_b} = \frac{D_e}{D_b} - C_0 \frac{u}{v^2} \quad (\text{A5})$$

$$\frac{\partial D_e}{\partial C_0} = -\frac{u}{v^2} D_b \quad (\text{A6})$$

$$\frac{\partial D_e}{\partial L_b} = 2j_s \frac{u}{v^2} \quad (\text{A7})$$

For the formation of the partial derivatives of equation 13, the latter equation is subdivided into expressions for the counter and denominator:

$$y = 6t_{bt} C_0 j_s D_b^2 \quad (\text{A8})$$

$$z = L_c C_0^2 D_b^2 + 2L_b L_c C_0 D_b j_s - 2L_b L_c j_s^2 \quad (\text{A9})$$

The partial derivatives of equation 13 are calculated as follows:

$$\frac{\partial \alpha}{\partial t_{bt}} = \frac{\alpha}{t_{bt}} \quad (\text{A10})$$

$$\frac{\partial \alpha}{\partial C_0} = \frac{\alpha}{C_0} - \frac{y}{z^2} (2L_c C_0 D_b^2 + 2L_b L_c D_b j_s) \quad (\text{A11})$$

$$\frac{\partial \alpha}{\partial D_b} = 2\alpha - \frac{y}{z^2} (2L_c D_b C_0^2 + 2L_b L_c C_0 j_s) \quad (\text{A12})$$

$$\frac{\partial \alpha}{\partial j_s} = \frac{\alpha}{j_s} - \frac{y}{z^2} (2L_b L_c C_0 D_b + 4L_c j_s L_b^2) \quad (\text{A13})$$

$$\frac{\partial \alpha}{\partial L_c} = -\frac{y}{z^2} (C_0^2 D_b^2 + 2L_b C_0 D_b j_s - 2L_b^2 j_s^2) \quad (\text{A14})$$

$$\frac{\partial \alpha}{\partial L_b} = -\frac{y}{z^2} (2L_c C_0 D_b j_s - 4L_b L_c j_s^2) \quad (\text{A15})$$